

Synthesis and characterisation of luminescent fluorinated organoboron compounds†

Juri Ugolotti, Sondra Hellstrom, George J. P. Britovsek,* Tim S. Jones,* Patricia Hunt and Andrew J. P. White

Received 9th January 2007, Accepted 8th February 2007

First published as an Advance Article on the web 28th February 2007

DOI: 10.1039/b700317j

The reaction of 8-hydroxyquinoline (HQ) with $B(C_6F_5)_3$ leads to the formation of the zwitterionic compound $(C_6F_5)_3BQH$ (**1**), involving a proton migration from O to N. Compound **1** can be converted thermally to $(C_6F_5)_2BQ$ (**2**), which can also be prepared from $(C_6F_5)_2BCl$ and HQ. The reaction of HQ with $(C_6F_5)B(OC_6F_5)_2$ generates initially $(C_6F_5)(OC_6F_5)BQ$ (**3**), which easily hydrolyses to give the diboron compound $((C_6F_5)BQ)_2O$ (**4**). Compounds **1**, **2** and **4** have been fully characterised, including X-ray analysis. The spectroscopic properties of these compounds, including photoluminescence (PL) have been investigated and compared with the non-fluorinated luminescent boron compound $(C_6H_5)_2BQ$ and also with AlQ_3 . The changes in luminescent behaviour upon fluorination of these boron quinolinate compounds have been rationalised using computational studies.

Introduction

Luminescent organic and organometallic compounds are currently of great interest due to their potential application in organic light emitting devices (OLEDs).¹ Since the original report by Tang and VanSlyke² on the electroluminescent properties of AlQ_3 (HQ = 8-hydroxyquinoline, see Fig. 1), many derivatives have been prepared with emission wavelengths now covering most of the visible region of the spectrum.^{3,4} More recently, luminescent organoboron compounds have received increased attention due to their better stability compared to aluminium compounds. Examples include mononuclear four-coordinate boron compounds of the type $R_2B(N,N)$ ^{4,9,10} and $R_2B(N,O)$,^{5–8} where N,N and N,O are bidentate heterocyclic ligands with one neutral N and one negative N or O donor, respectively, for example Ph_2BQ (Fig. 1). In addition, some luminescent oxygen-bridged diboron compounds have been reported recently.^{11,12}

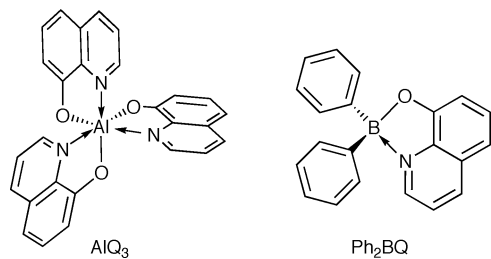


Fig. 1 Examples of luminescent aluminium and boron compounds.

Various derivatives of these boron-based emitters have been prepared, most of which are variations on the N,O or N,N part of the molecule, whereby substituents on the heterocycle affect the HOMO–LUMO levels and thereby the colour of the emission.⁹

Department of Chemistry, Imperial College London, Exhibition Road, London, SW7 2AY, UK. E-mail: g.britovsek@imperial.ac.uk; t.jones@imperial.ac.uk; Tel: +44-(0)20-75945863; +44-(0)20-75945794

† Electronic supplementary information (ESI) available: Molecular structures of compounds **1**, **2** and **4** (Fig. S1–S6). See DOI: 10.1039/b700317j

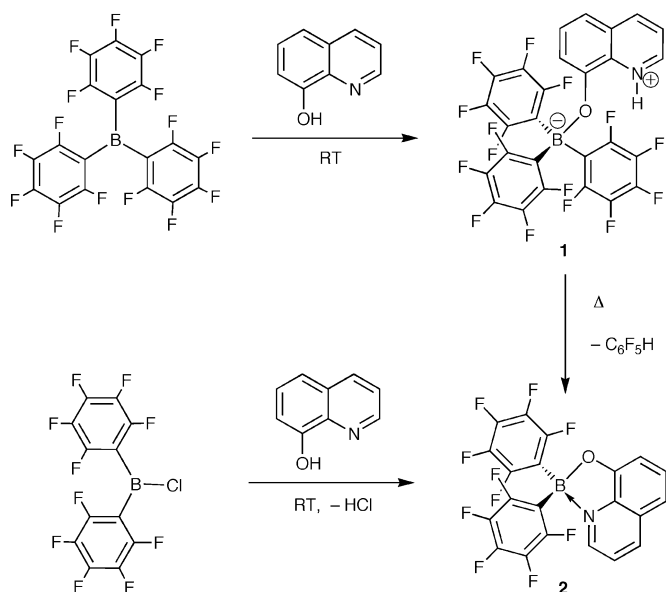
An alternative method for tuning the emission wavelength and the quantum yield might be to vary the R substituents at the boron centre. Thus far, the R groups have been generally phenyl or electronically similar groups such as naphthyl,⁵ thienyl or benzothenyl.⁶ Changing the electron-withdrawing or electron-donating properties of the R substituents will affect the Lewis acidity of the boron centre, which in turn may affect the boron–quinoline interaction and thereby the HOMO–LUMO levels. In order to explore this possibility, we decided to prepare a series of pentafluorophenyl substituted boron quinolyl compounds of the general formula $(C_6F_5)_{2-n}(OC_6F_5)_nBQ$ where $n = 0, 1$ or 2 . Compared to a phenyl group, the electron-withdrawing C_6F_5 groups will increase the Lewis acidity of the boron centre and thereby affect the energy of the HOMO–LUMO levels, which are located on the quinoline moiety of the molecule. Pentafluorophenyl groups may also offer an advantage in terms of stability, *cf.* $B(C_6F_5)_3$ is considerably less air and moisture sensitive compared to $B(C_6H_5)_3$ due to the increased steric protection of the Lewis acidic boron centre.¹³ This, however, does not apply to compounds containing BOC_6F_5 groups, which are much more susceptible to hydrolysis.^{14,15} Fluorination may also increase the volatility of the precursors, which may prove beneficial in device formation. A few studies on the effect of fluorination have been reported but these were all on fluorination of the fluorescent heterocyclic part of the molecule.^{9,16,17} We report here the synthesis and characterisation of a series of novel fluorinated quinolyl boron compounds and an experimental and computational assessment of the effects of fluorination on their luminescent properties.

Results and discussion

Synthesis of organoboron compounds

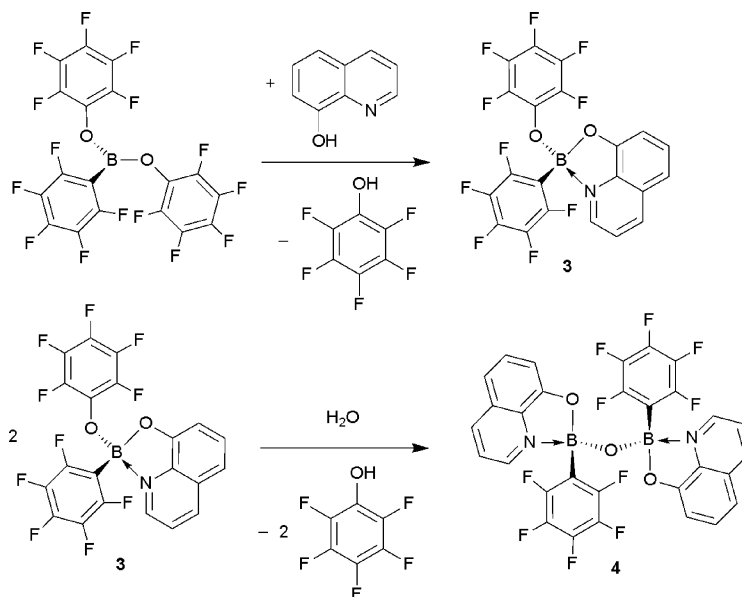
The reaction of 8-hydroxyquinoline (HQ) with BPh_3 has been reported to proceed smoothly at room temperature within several hours to give Ph_2BQ and benzene.⁵ In contrast, we found that the reaction of $B(C_6F_5)_3$ with HQ at room temperature results in the formation of the zwitterionic adduct $(C_6F_5)_3BQH$

(1), whereby the oxygen is coordinated to the boron centre and a proton shift from oxygen to nitrogen has occurred (Scheme 1). Interestingly, a similar proton shift has been observed in the reaction between $B(C_6F_5)_3$ and α -naphthol, whereby a proton migrates from oxygen to the *para*-carbon centre upon coordination of boron to oxygen.¹⁸ The adduct **1** can be converted to the bis(pentafluorophenyl)boronic acid quinolyl ester ($C_6F_5)_2BQ$ (**2**) by refluxing **1** in benzene, concomitant with the loss of pentafluorobenzene. Alternatively, **2** can be prepared by reacting $(C_6F_5)_2BCl$ with 8-hydroxyquinoline at room temperature in CH_2Cl_2 for 2 h (Scheme 1).



Scheme 1

The preparation of (pentafluorophenyl)boronic acid pentafluorophenyl quinolyl ester ($C_6F_5)(OC_6F_5)BQ$ (**3**) was carried out by reacting $(C_6F_5)B(OC_6F_5)_2$ with 8-hydroxyquinoline (Scheme 2).



Scheme 2

This compound is much more moisture sensitive compared to **2** due to the ease of hydrolysis of the remaining pentafluorophenoxy moiety. Indeed, dissolution of compound **3** in normal grade hexane resulted in the formation of the dimeric product $((C_6F_5)BQ)_2O$ (**4**), together with the loss of pentafluorophenol. The synthesis and electroluminescent properties of a similar non-fluorinated analogue $((C_6H_5)BQ)_2O$ were recently reported ($Q' = 2$ -methyl-8-hydroxyquinoline).¹¹

In analogy to the formation of compound **3**, the reaction of $B(OC_6F_5)_3$ with 8-hydroxyquinoline was expected to produce the boric acid ester $(F_5C_6O)_2BQ$ (**5**). However, this product could never be isolated with acceptable purity as all attempts resulted in the formation of by-products, probably the dimeric compound $((F_5C_6O)BQ)_2O$ and further degradation products due to hydrolysis of the BOC_6F_5 moieties.

All compounds **1–4** are bright yellow solids, which show fluorescence in solution and the solid state. They have been characterised by 1H , ^{19}F and ^{11}B NMR spectroscopy, MS, CHN analysis as well as solution UV-vis and PL spectroscopy. The solid state structures of compounds **1**, **2** and **4** have been determined by X-ray crystallography. The energies of the HOMO and LUMO levels for compounds **1**, **2** and **4** and the corresponding excitation energies have been determined computationally and compared with experimental values.

Solid state structures

The X-ray analysis of crystals of compound **1** revealed the presence of two independent molecules (I and II) in the asymmetric unit; molecule I is shown in Fig. 2, and molecule II in Fig. S2 in the ESI.† The conformations of the two molecules are distinctly dissimilar; while the $OB(C_6F_5)_3$ portions are very comparable (having an r.m.s. fit of *ca.* 0.12 Å), the quinoline rings adopt noticeably different orientations (see Fig. S4†), the torsion angle about the C–O bond being *ca.* +30 and -5° in molecules I and II respectively. The 8-quinolinol ring has adopted a monodentate *O*-coordination mode to the boron centre rather than a bidentate *N,O* mode, which

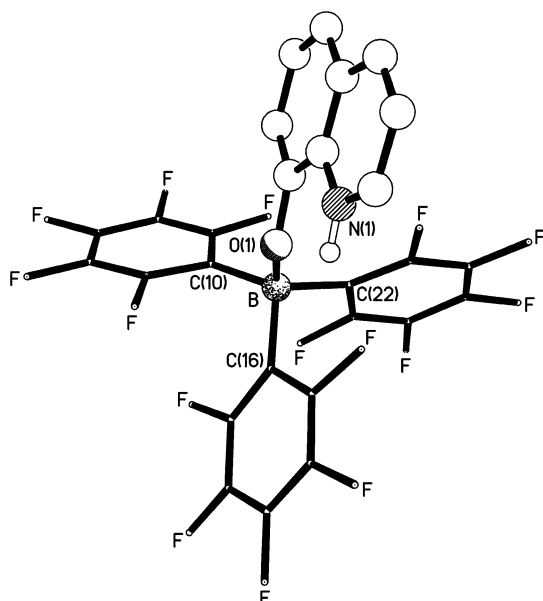


Fig. 2 The molecular structure of one (I) of the two independent molecules present in the crystals of $(\text{C}_6\text{F}_5)_3\text{BQH}$ (**1**).

appears to be the first such example for a 8-quinolinol ring linked to a boron atom. The geometry at the boron centre is distorted tetrahedral with angles in the range $103.2(2)$ – $115.6(2)^\circ$ and $103.8(2)$ – $113.9(2)^\circ$ for molecules I and II respectively. In both cases the B–O bond length is significantly shorter than the B–C bonds (Table 1). The N–H proton in each independent molecule is involved in intermolecular N–H \cdots F hydrogen bonding to a symmetry-related counterpart. For molecule I the proton links to an *ortho* fluorine [F(15)] on the C(10) pentafluorophenyl ring in a C_i -related neighbour [N \cdots F 2.929(3) Å, H \cdots F 2.27 Å, N–H \cdots F 130°], and *vice versa* to give centrosymmetric dimer pairs. For molecule II, by contrast, the proton donates to a *meta* fluorine [F(14')] on the C(10) ring in a glide related counterpart [N \cdots F 2.938(3) Å, H \cdots F 2.33 Å, N–H \cdots F 124°] giving rise to

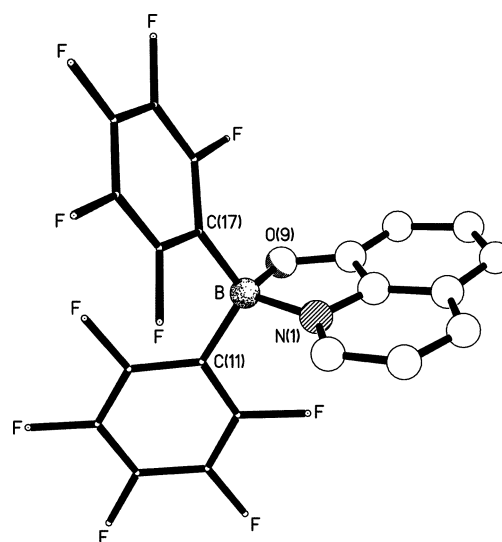


Fig. 3 The molecular structure of $(\text{C}_6\text{F}_5)_2\text{BQ}$ (**2**).

Table 1 Selected bond lengths (Å) and angles ($^\circ$) for **1**

	Molecule I	Molecule II		Molecule I	Molecule II
B–O(1)	1.508(4)	1.491(4)	B–C(10)	1.654(5)	1.659(5)
B–C(16)	1.664(4)	1.666(4)	B–C(22)	1.656(5)	1.655(4)
O(1)–B–C(10)	107.8(2)	107.7(2)	O(1)–B–C(16)	103.2(2)	104.0(2)
O(1)–B–C(22)	112.9(3)	113.8(2)	C(10)–B–C(16)	112.7(3)	113.3(2)
C(10)–B–C(22)	115.6(2)	113.9(2)	C(16)–B–C(22)	104.0(2)	103.8(2)

Table 2 Selected bond lengths (Å) and angles ($^\circ$) for $(\text{C}_6\text{F}_5)_2\text{BQ}$ (**2**) and the two independent molecules in its bis(phenyl) analogue $(\text{C}_6\text{H}_5)_2\text{BQ}$ ¹⁹

	2	$(\text{C}_6\text{H}_5)_2\text{BQ}$ molecule I	$(\text{C}_6\text{H}_5)_2\text{BQ}$ molecule II
B–N(1)	1.637(2)	1.61(1)	1.61(1)
B–O(9)	1.494(2)	1.56(1)	1.54(1)
B–C(11)	1.624(3)	1.59(1)	1.59(1)
B–C(17)	1.629(3)	1.58(1)	1.58(1)
N(1)–B–O(9)	99.43(13)	96.6(7)	96.7(8)
N(1)–B–C(11)	111.35(14)	111.1(8)	109.5(9)
N(1)–B–C(17)	107.64(14)	111.1(8)	109.7(8)
O(9)–B–C(11)	108.26(14)	109.2(8)	110.8(8)
O(9)–B–C(17)	111.90(15)	109.0(8)	110.2(9)
C(11)–B–C(17)	116.89(15)	117.7(9)	117.9(9)

an extended chain of molecules along the crystallographic *b*-axis direction.

The solid state structure of **2** (Fig. 3), where the 8-quinolinol ring coordinates in a bidentate *N,O* fashion, is very similar to the structure of the unfluorinated bis(phenyl) analogue $(\text{C}_6\text{H}_5)_2\text{BQ}$, which has two independent molecules in the solid state.¹⁹ Despite the rather high estimated standard deviations (esds) for both independent molecules in $(\text{C}_6\text{H}_5)_2\text{BQ}$, it is possible to see the differences in the boron coordination geometry caused by having pentafluorophenyl rather than phenyl rings. The B–O bond in **2** [1.494(2) Å] is shorter [1.56(1) and 1.54(1) Å], whilst the B–C bonds in **2** [1.624(3) and 1.629(3) Å] are longer than those in $(\text{C}_6\text{H}_5)_2\text{BQ}$ [in the range 1.58(1)–1.59(1) Å]. For the B–N bonds, the large esds in $(\text{C}_6\text{H}_5)_2\text{BQ}$ make the apparent lengthening in **2** not significant (Table 2). The most notable feature of the angles at the boron centre is an enlargement of *ca.* 3° in **2** for the O–B–N

bite angle, a consequence of the contracted B–O bond length. The five-membered chelate ring in **2** adopts a slight envelope conformation, the boron lying *ca.* 0.14 Å out of the C₂NO plane (which is coplanar to better than 0.01 Å) in the direction of C(17).

The crystal structure of **4** shows the oxygen-bridged complex to have molecular C₂ symmetry about an axis that passes through the bridging oxygen and bisects the B–O–B angle (Fig. 4). The two boron centres have very similar geometries (Table 3), and it is notable that in each case the B–O bonds to the bridging oxygen O(3) [1.406(4) and 1.397(3) Å for B(1) and B(2) respectively] are *ca.* 0.10 Å shorter than those to the oxygens of the chelating 8-quinolinol rings [1.507(3) and 1.518(3) Å for B(1) and

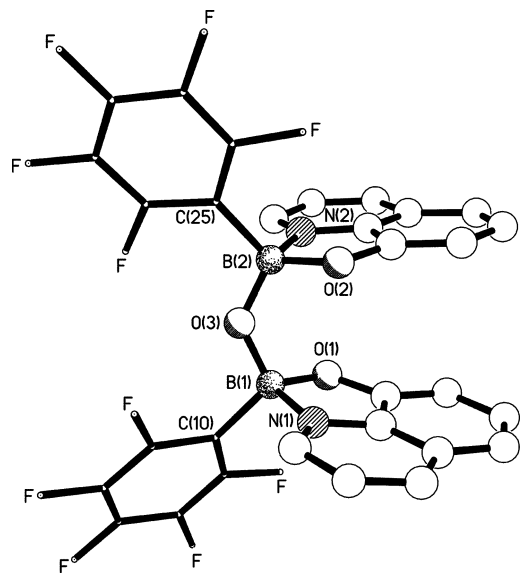


Fig. 4 The molecular structure of ((C₆F₅)₂BQ)₂O **4**.

Table 3 Selected bond lengths (Å) and angles (°) for **4** and its closely related phenyl analogue ((C₆H₅)₂BQ)₂O^{11a}

	4	((C ₆ H ₅) ₂ BQ) ₂ O
B(1)–O(1)	1.507(3)	1.522(5), 1.526(5)
B(2)–O(2)	1.518(3)	
B(1)–N(1)	1.648(4)	1.670(5), 1.672(5)
B(2)–N(2)	1.652(4)	
B(1)–C(10)	1.641(4)	1.612(6), 1.609(6)
B(2)–C(25)	1.633(4)	
B(1)–O(3)	1.406(4)	1.397(5), 1.392(5)
B(2)–O(3)	1.397(3)	
O(1)–B(1)–N(1)	98.57(18)	97.3(3), 96.8(3)
O(2)–B(2)–N(2)	98.10(18)	
O(1)–B(1)–C(10)	112.5(2)	111.5(3), 110.8(3)
O(2)–B(2)–C(25)	112.2(2)	
N(1)–B(1)–O(3)	112.1(2)	110.9(3), 110.7(3)
N(2)–B(2)–O(3)	111.2(2)	
N(1)–B(1)–C(10)	108.2(2)	109.1(3), 109.6(3)
N(2)–B(2)–C(25)	108.9(2)	
O(3)–B(1)–C(10)	111.2(2)	112.6(3), 113.2(3)
O(3)–B(2)–C(25)	111.7(2)	
O(1)–B(1)–O(3)	113.6(2)	114.3(3), 114.6(3)
O(2)–B(2)–O(3)	113.9(2)	
B(1)–O(3)–B(2)	128.2(2)	129.8(3)

^a Due to the molecular C₂ symmetry possessed by both species the bond lengths and angles have been grouped together on the basis of this pseudo symmetry.

B(2) respectively]. The five-membered chelate rings have planar conformations [C₂NOB coplanar to within *ca.* 0.01 and 0.02 Å for the B(1)- and B(2)-containing rings respectively] with O–B–N bite angles of 98.57(18) and 98.10(18)° at B(1) and B(2) respectively. The two 8-quinolinol rings are inclined to each other by *ca.* 16°, and are oriented such that there is very little overlap between them; considering the view in Fig. 4, the O(1)/N(1) ring system is positioned out of the plane of the paper (towards the viewer) whilst the O(2)/N(2) ring system is positioned into this same plane (away from the viewer). The closest analogue for complex **4** is (μ₂-oxo)-bis((2-methyl-8-quinolinolato)phenylborane ((C₆H₅)₂BQ)₂O where Q' has a methyl group in the 2-position of each 8-quinolinol ring, and phenyl instead of pentafluorophenyl groups.¹¹ The parameters for this compound along with those for complex **4** are given in Table 3. Unfortunately, the differences are not large enough compared to the esds to be considered significant.

UV-vis and photoluminescence (PL) spectroscopy

The UV-vis spectra for compounds **2** and **4** have been measured in CH₂Cl₂ solution and the λ_{max} and ε_{max} values are collected in Table 4, together with those determined for AlQ₃ and (C₆H₅)₂BQ. For comparison, we have also included values reported by others for AlQ₃ and (C₆H₅)₂BQ. It can be seen that compared to the non-fluorinated compound (C₆H₅)₂BQ, only a slight blue shift of the absorption maximum λ_{max} is observed for compound **2**, which could be due to the increased Lewis acidity of the boron centre. In the case of the oxo-bridged compound **4**, which displays a similar λ_{max} as (C₆H₅)₂BQ, the Lewis acidity of the boron centres is likely to be reduced due to the donating ability of the bridging oxygen atom. Overall, considering the variation in λ_{max} values, fluorination seems to have only a small effect on the position and intensity of the absorption maximum in the UV-vis spectra.

The PL spectra were determined in CH₂Cl₂ solution and are shown in Fig. 5. Again, there appears to be very little difference in the peak emission wavelength between the non-fluorinated and fluorinated boron compounds. However, the quantum yield appears to be affected by fluorination. The relative quantum yield of (C₆H₅)₂BQ was found to be 2.5 times better than AlQ₃, which correlates well with previous reports.⁷ For the fluorinated compound **2**, the relative quantum yield was found to be 1.8 times that of AlQ₃.

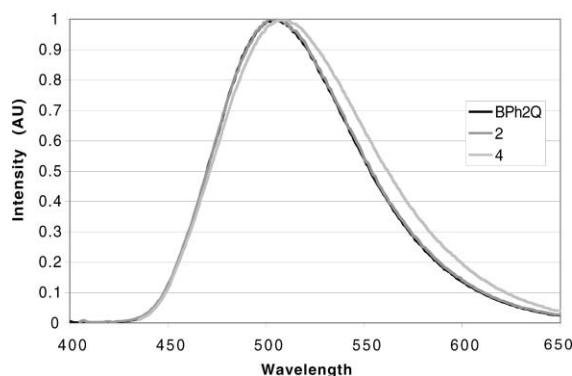


Fig. 5 Photoluminescence (PL) spectra for compounds Ph₂BQ, **2** and **4** in CH₂Cl₂.

Table 4 Physical properties of compounds $(C_6F_5)_2BQ$ **2** and $((C_6F_5)BQ)_2O$ **4**

Compound	NMR ^a	UV-vis ^b		PL ^b	Reference
	¹¹ B (ppm)	λ_{max}/nm	$\epsilon_{max}/M^{-1} cm^{-1}$	λ_{max}/nm	
AlQ ₃		387	10000	516	8
		390		514	20
		387 ^c		515 ^c	17
		384 ^c		517 ^c	21
		383 ^b		524 ^b	22
$(C_6H_5)_2BQ$		387	6600	530	This work
		395		505	8
		396	3200	504	7
		400 ^c		497 ^c	21
$(C_6F_5)_2BQ$ 2	11.1	395	8440	515	This work
$((C_6F_5)BQ)_2O$ 4	7.0	389	6600	515	This work
$((C_6H_5)BQ)_2O$	8.5	395		508	This work
	10.35	319 ^c		496 ^c	11

^a Measured in CDCl₃. ^b Measured in CH₂Cl₂. ^c Measured in CHCl₃.

Computational studies

In order to explain the results from the luminescence studies, a computational study was carried out on the compounds $(C_6H_5)_2BQ$, **2** and **4**, both in the gas phase and in dichloromethane solution. The effects of solvation have been mimicked by placing the solute within a cavity (large or small) in a polarisable medium that responds to the local charge distribution of the solute (see Experimental). The calculations have shown that fluorination of the phenyl rings at the boron centre has the effect of decreasing, *i.e.* stabilising, both the HOMO and LUMO energy levels of these compounds, as depicted in Fig. 6. The largest stabilisation occurs

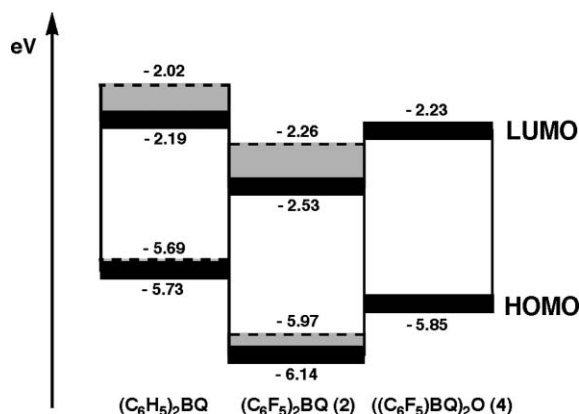


Fig. 6 Difference in energy between the HOMO and LUMO levels of Ph_2BQ , **2** and **4**. The dashed lines represent MO energy levels for the small cavity solvent model and the solid lines the MO energy levels for the large cavity solvent model.

in compound **2**. In compound **4**, the stabilisation is reduced because each boron centre is bonded to only one pentafluorophenyl group, but it is still noticeably larger compared to $(C_6H_5)_2BQ$.

In luminescent compounds containing 8-quinolinolate groups, the HOMO and LUMO are localised on the 8-quinolinolate group, primarily on the phenoxy and pyridyl part, respectively.^{7,8,23} This is also the case for **2** and **4**. The delocalised HOMO and LUMO orbitals for **4** are shown in Fig. 7.

We have also computed the three lowest electronic excitation energies (vertical) for the singlet states of each compound. TD-DFT calculations were performed on geometries optimised at the B3LYP/6-31G(d) level in the gas phase and with dichloromethane as a solvent. In order to compare our results with previous studies,²³ we have also computed the TD-DFT excitation energies for the HF optimised geometry of $(C_6H_5)_2BQ$. Absorption wavelengths of 406 and 404 nm (see Table 5) were obtained for $(C_6H_5)_2BQ$ and **2**, respectively, using the small cavity solvation model, which are in reasonable agreement with the experimental values of 395 and 389 nm (Table 4) and are also comparable with those reported previously for $(C_6H_5)_2BQ$.²³ The excitation wavelengths for the HF structure of $(C_6H_5)_2BQ$ are *ca.* 20 nm lower than those computed using the DFT-B3LYP structure, consistent with the findings of Teng *et al.*²³ Compound **4** could not be optimised within the small cavity model and we therefore investigated the large cavity model, resulting in a rather large excitation wavelength of 411 nm. It was noticed that the use of the large cavity model increases the first excitation wavelength by an average of 16 nm for $(C_6H_5)_2BQ$ and **2**. A correction of -16 nm applied to the large cavity result (411 nm) produces an estimate of 395 nm for the first singlet excitation wavelength of **4**, which matches exactly the experimentally determined value.

Table 5 Excitation energies (nm) and oscillator strength in brackets for the three singlet states of $(C_6H_5)_2BQ$, $(C_6F_5)_2BQ$ (**2**) and $((C_6F_5)BQ)_2O$ (**4**)

	$(C_6H_5)_2BQ$ HF ^a	$(C_6H_5)_2BQ$ B3LYP ^a	$(C_6F_5)_2BQ$ (2) B3LYP ^a	$((C_6F_5)BQ)_2O$ (4) B3LYP ^b
S 1	385 (0.08)	406 (0.09)	404 (0.07)	411 (0.06)
S 2	316 (0.008)	334 (0.005)	321 (0.0003)	402 (0.03)
S 3	307 (0.008)	323 (0.01)	316 (0.0005)	390 (0.03)

^a A dichloromethane polarisable continuum model was used. ^b A large cavity was employed.

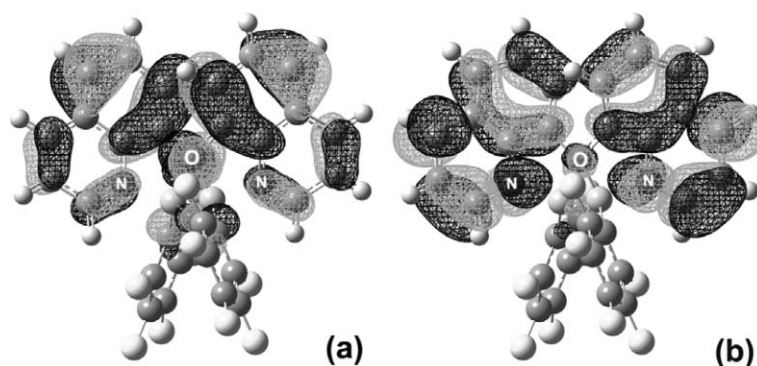


Fig. 7 (a) HOMO and (b) LUMO orbitals of $((\text{C}_6\text{F}_5)_2\text{BQ})_2\text{O}$ (**4**). Light areas have positive phase and dark areas negative phase, depicted for an isovalue of 0.02.

In conclusion, the experimental and computational studies on the spectroscopic and luminescent properties of the boron quinolinolate compounds $(\text{C}_6\text{H}_5)_2\text{BQ}$, **2** and **4** have shown that fluorination of the phenyl rings results in a stabilisation of both the HOMO and LUMO levels and therefore the effect on the absorption and emission maxima in the UV-vis and PL spectra, respectively, is only minimal. However, the difference in stability and volatility between fluorinated and unfluorinated luminescent boron compounds may have an effect on their solid state properties and their performance in OLED devices, which will be the subject of future investigations. The good agreement between the computational and experimental results has shown that modest B3LYP/6-31G(d) calculations (which include basic solvation effects) can be used to offer valuable insights into factors affecting absorbance and emittance, and may potentially be used as a predictive tool for similar compounds.

Experimental

General

All moisture-sensitive compounds were manipulated using standard vacuum line, Schlenk or cannula techniques, or in a conventional nitrogen-filled glove box. ^1H , ^{19}F and ^{11}B NMR spectra were recorded on a Bruker AC-250 or a Jeol JNM-EX270 spectrometer; chemical shifts for ^1H and ^{13}C NMR are referenced to the residual protio impurity and to the ^{13}C NMR signal of the deuterated solvent. ^{19}F and ^{11}B chemical shifts are reported relative to CFCl_3 and $\text{BF}_3 \cdot \text{OEt}_2$, respectively. Elemental analyses were performed by the Science Technical Support Unit at the London Metropolitan University. Absorption spectra were measured using a Perkin Elmer UV-Vis Lambda-2 spectrometer. PL spectra were measured using a Jobin-Yvon Fluorolog-3 with an integration time of 1.0 s and monochromator slits set at 1 nm. All solution state spectra were obtained from 10^{-5} M solutions in dry CH_2Cl_2 ; measurements were taken in right-angle mode. All spectra were taken in 5 nm intervals and corrected against dark counts and detector factors. Relative PL efficiency is calculated using the formula

$$\frac{Q_{1-3}}{Q_{\text{AIQ3}}} = \frac{OD_{\text{AIQ3}}}{I_{\text{AIQ3}}} \frac{I_{1-3}}{OD_{1-3}}$$

where Q is the PL efficiency, I is the integral of the corresponding PL spectrum from 400–750 nm and OD is the optical density of

the relevant sample at the excitation wavelength of 396 nm. For each compound, data is taken for six optical densities all less than 0.1 and the fraction I/OD is calculated as the slope of the best-fit line through these points.

Computational details

All calculations were performed using the *Gaussian 03* program package.²⁴ Structures were optimised at the HF and DFT levels, and confirmed as minima by frequency analysis. We have employed the B3LYP hybrid functional^{25,26} which has recently been shown to perform reasonably well for these types of compounds.^{9,17,23,27} Both 6-31G(d) and 6-31G(d,p) basis sets have been tested.^{28,29} Very similar results were obtained with both sets and we have therefore used the smaller 6-31G(d) basis set because of the faster computational times. Excitation energies have been calculated for the fully optimised DFT-B3LYP (or HF) structures using time-dependent (TD) DFT.³⁰⁻³² The effects of a solvent, dichloromethane, were included in an approximate way by employing the polarisable conductor-like screening model implemented in Gaussian (C-PCM).³³⁻³⁵ For the “small cavity model” the cavity surface is determined using spheres placed around each heavy atom of the solute (hydrogen atoms are enclosed in the sphere of the atom to which they are bonded). However, optimisation of $((\text{C}_6\text{F}_5)_2\text{BQ})_2\text{O}$ (**4**) in the solvent proved problematic because of the proximity of the two nearly-parallel 8-quinolinolate groups, hence a “large cavity model” was employed where the cavity volume is increased by adding the radius of the solvent to the radii of the solute atoms. The HOMO and LUMO values for $(\text{C}_6\text{H}_5)_2\text{BQ}$ and $(\text{C}_6\text{F}_5)_2\text{BQ}$ (**2**) are therefore reported as an energy band in Fig. 6 rather than an energy level, because they are calculated with both solvent models. A single value is reported for $((\text{C}_6\text{F}_5)_2\text{BQ})_2\text{O}$ (**4**), because only the large cavity model would converge.

Solvents and reagents

Toluene and pentane were dried by passing through a column, filled with commercially available Q-5 reagent (13 wt% CuO on alumina) and activated alumina (pellets, 3 mm). Dichloromethane and acetonitrile were dried over CaH_2 and distilled under nitrogen. The synthesis of $\text{B}(\text{C}_6\text{F}_5)_3$,¹³ $(\text{C}_6\text{F}_5)_2\text{BCl}$,³⁶ $(\text{C}_6\text{F}_5)\text{B}(\text{OC}_6\text{F}_5)_2$,¹⁴ $\text{B}(\text{OC}_6\text{F}_5)_3$ ³⁷ and $(\text{C}_6\text{H}_5)_2\text{BQ}$ ⁵ have been reported previously. All

other chemicals and NMR solvents were obtained commercially and used as received.

Quinolinium tris(pentafluorophenyl)borate (C₆F₅)₃B(OC₉H₆NH) (1). B(C₆F₅)₃ (100 mg, 0.19 mmol) and 8-hydroxyquinoline (28 mg, 0.19 mmol) were placed together into a Schlenk flask and dissolved in 40 mL of CH₂Cl₂. The colour of the solution was bright yellow. The solution was stirred at room temperature for 1 h, after which the solvent was removed under reduced pressure, leaving the product as a yellow solid. Crystals suitable for single crystal X-ray diffraction were obtained in hexane at room temperature.

¹H NMR (ppm, CDCl₃, 250 MHz): 8.95 (d, ³J = 8.2 Hz, 1 H), 8.83 (t, ³J = 6.4 Hz, 1 H), 7.96 (t, ³J = 5.4 Hz, 1 H), 7.66 (t, ³J = 8.3 Hz, 1 H), 7.48 (d, ³J = 8.3 Hz, 1 H), 7.04 (d, ³J = 8.2 Hz, 1 H). ¹⁹F NMR (ppm, CDCl₃, 235 MHz): -135.0 (*o*-F), -159.7 (*p*-F), -165.1 (*m*-F). ¹¹B NMR (ppm, CDCl₃, 86 MHz): -3.1. Elemental analysis (calc. for (C₆F₅)₃B(OC₉H₆NH)): C = 49.35, H = 1.07, N = 2.13%; C = 49.33, H = 1.03, N = 2.17%.

Bis(pentafluorophenyl)borinic acid quinolyl ester (C₆F₅)₂-B(OC₉H₆N) (2). (C₆F₅)₂BCl (150 mg, 0.394 mmol) and 8-hydroxyquinoline (57 mg, 0.394 mmol) were placed into a Schlenk flask and dissolved in 50 mL of CH₂Cl₂. The solution, which was bright yellow, was stirred under nitrogen for 2 h, after which the solvent was removed by high vacuum, leaving a yellow solid (yield = 91%). Crystals suitable for single crystal X-ray diffraction were obtained in hexane at room temperature. ¹H NMR (ppm, CDCl₃, 250 MHz): 8.85 (d, ³J = 5.3 Hz, 1 H), 8.56 (d, ³J = 8.2 Hz, 1 H), 7.78-7.67 (m), 7.39 (d, ³J = 8.2 Hz, 1 H), 7.21 (d, ³J = 7.6 Hz, 1 H). ¹⁹F NMR (ppm, CDCl₃, 235 MHz): -135.4 (*o*-F), -156.0 (*p*-F), -163.3 (*m*-F). ¹¹B NMR (ppm, CDCl₃, 86 MHz): 7.0. MS-EI+ (*m/z*): 489 ([M]⁺ 322 ([M-C₆F₅]⁺). Elemental analysis (calc. for (C₆F₅)₂B(OC₉H₆N)): C = 51.57, H = 1.24, N = 2.86%; C = 51.53, H = 1.20, N = 2.79%.

Pentafluorophenylboronic acid quinolyl pentafluorophenyl ester (C₆F₅)₃B(OC₉H₆N)(OC₆F₅) (3). (C₆F₅)₃B(OC₆F₅)₂ (300 mg, 0.55 mmol) was placed in a Schlenk flask together with 8-hydroxyquinoline (80 mg, 0.55 mmol). After the addition of 50 mL of CH₂Cl₂ to the flask, a bright yellow solution was produced. After 1 h stirring, the solvent was removed by reduced pressure, leaving a bright yellow powder. The product was dissolved in hot hexane and left at 4 °C overnight. The day after, the yellow precipitate was filtered and washed with hexane, resulting in 97 mg of product **3** (yield = 56%). ¹H NMR (ppm, CDCl₃, 250 MHz): 8.93 (d, ³J = 5.1 Hz, 1 H), 8.62 (d, ³J = 8.3 Hz, 1 H), 7.86-7.81 (m), 7.68 (t, ³J = 7.7 Hz, 1 H), 7.40 (d, ³J = 8.3 Hz, 1 H), 7.16 (d, ³J = 7.7 Hz, 1 H). ¹⁹F NMR (ppm, CDCl₃, 235 MHz): -134.3 (*o*-F, C₆F₅), -155.2 (*p*-F, C₆F₅), -157.2 (*o*-F, OC₆F₅), -163.3 (*m*-F, C₆F₅), -165.3 (*m*-F, OC₆F₅), -166.8 (*p*-F, OC₆F₅). ¹¹B NMR (ppm, CDCl₃, 86 MHz): 8.4. Elemental analysis (calc. for (C₆F₅)₃(OC₆F₅)B(OC₉H₆N)): C = 49.94, H = 1.20, N = 2.77%; C = 49.84, H = 1.12, N = 2.66%.

Pentafluorophenyl(8-quinolinolate)borinic anhydride ((C₆F₅)₂-BQ)₂O (4). Attempts to grow crystals suitable for single crystal X-ray diffraction of compound **3** from hexane at 4 °C resulted in the formation of compound **4**, probably due to small amounts of water in the solvent. Crystals of compound **4** were analysed by X-ray crystallography and NMR spectroscopy. ¹⁹F NMR (ppm,

Table 6 Crystallographic data for compounds **1**, **2** and **4**^a

Data	1	2	4
Chemical formula	C ₂₇ H ₇ BF ₁₅ NO	C ₂₁ H ₆ BF ₁₀ NO	C ₃₀ H ₁₂ B ₂ F ₁₀ N ₂ O ₃
Solvent	0.5CH ₂ Cl ₂	—	—
FW	699.61	489.08	660.04
<i>T</i> /°C	-100	-100	-100
Space group	<i>C</i> 2/ <i>c</i> (no. 15)	<i>P</i> 2 ₁ / <i>c</i> (no. 14)	<i>P</i> 1̄ (no. 2)
<i>a</i> /Å	26.9700(11)	15.3409(13)	8.0303(8)
<i>b</i> /Å	10.5284(4)	7.8053(6)	12.2898(12)
<i>c</i> /Å	37.9995(14)	15.4746(14)	13.6929(15)
<i>α</i> /°	—	—	86.956(8)
<i>β</i> /°	104.723(3)	96.164(7)	89.875(9)
<i>γ</i> /°	—	—	85.670(8)
<i>V</i> /Å ³	10435.7(7)	1842.2(3)	1345.6(2)
<i>Z</i>	16 ^b	4	2
<i>ρ</i> _{calcd} /g cm ⁻³	1.781	1.763	1.629
<i>λ</i> /Å	1.54248	1.54248	1.54248
<i>μ</i> /mm ⁻¹	2.561	1.605	1.342
<i>R</i> ₁ ^c	0.051	0.035	0.050
<i>wR</i> ₂ ^d	0.130	0.086	0.099

^a Oxford Diffraction Xcalibur PX Ultra diffractometer, Cu K α radiation, refinement based on *F*². ^b There are two crystallographically independent molecules in the asymmetric unit. ^c *R*₁ = $\sum ||F_o| - |F_c|| / \sum |F_o|$. ^d *wR*₂ = $\{\sum [w(F_o^2 - F_c^2)^2] / \sum [w(F_o^2)^2]\}^{1/2}$; *w*⁻¹ = $\sigma^2(F_o^2) + (aP)^2 + bP$.

CDCl₃, 235 MHz): -135.2 (*o*-F), -156.1 (*p*-F), -164.5 (*m*-F). ¹¹B NMR (ppm, in CDCl₃, 86 MHz): 8.5.

Crystallographic details

Table 6 provides a summary of the crystallographic data for compounds **1**, **2** and **4**.

CCDC reference numbers 619418, 632949 and 632950.

For crystallographic data in CIF or other electronic format see DOI: 10.1039/b700317j

Acknowledgements

We are grateful to the EPSRC for financial support (GR/R92042/01).

References

- 1 *Organic Light Emitting Devices*, ed. K. Müllen and U. Scherf, Wiley-VCH, Weinheim, 2005.
- 2 C. W. Tang and S. A. VanSlyke, *Appl. Phys. Lett.*, 1987, **51**, 913.
- 3 C. H. Chen and J. Shi, *Coord. Chem. Rev.*, 1998, **171**, 161.
- 4 S. Wang, *Coord. Chem. Rev.*, 2001, **215**, 79.
- 5 Q. Wu, M. Esteghamatian, N.-X. Hu, Z. Popovic, G. Enright, Y. Tao, M. D'Iorio and S. Wang, *Chem. Mater.*, 2000, **12**, 79.
- 6 Y. Qin, C. Pagba, P. Piotrowiak and F. Jäkle, *J. Am. Chem. Soc.*, 2004, **126**, 7015.
- 7 Y. Cui, Q.-D. Liu, D.-R. Bai, W.-L. Jia, Y. Tao and S. Wang, *Inorg. Chem.*, 2005, **44**, 601.
- 8 S. Anderson, M. S. Weaver and A. J. Hudson, *Synth. Met.*, 2000, **111-112**, 459.
- 9 Q.-D. Liu, M. S. Mudadu, R. Thummel, Y. Tao and S. Wang, *Adv. Funct. Mater.*, 2005, **15**, 143.
- 10 Q.-D. Liu, M. S. Mudadu, H. Schmider, R. Thummel, Y. Tao and S. Wang, *Organometallics*, 2002, **21**, 4743.
- 11 H. J. Son, H. Jang, B.-J. Jung, D.-H. Kim, C. H. Shin, K. Y. Hwang, H.-K. Shim and Y. Do, *Synth. Met.*, 2003, **137**, 1001.
- 12 Q. Wu, M. Esteghamatian, N.-X. Hu, Z. Popovic, G. Enright, S. R. Breeze and S. Wang, *Angew. Chem., Int. Ed.*, 1999, **38**, 985.
- 13 A. G. Massey and A. J. Park, *J. Organomet. Chem.*, 1964, **2**, 245.

- 14 G. J. P. Britovsek, J. Ugolotti and A. J. P. White, *Organometallics*, 2005, **24**, 1685.
- 15 D. C. Bradley, I. S. Harding, A. D. Keefe, M. Motevalli and D. H. Zheng, *J. Chem. Soc., Dalton Trans.*, 1996, 3931.
- 16 M. Matsumura and T. Akai, *Jpn. J. Appl. Phys.*, 1996, **35**, 5357.
- 17 Y.-W. Shi, M.-M. Shi, J.-C. Huang, H.-Z. Chen, M. Wang, X. D. Liu, Y.-G. Ma, H. Xu and B. Yang, *Chem. Commun.*, 2006, 1941.
- 18 D. Vagedes, R. Froehlich and G. Erker, *Angew. Chem., Int. Ed.*, 1999, **38**, 3362.
- 19 H. Höpfl, V. Barba, G. Vargas, N. Farfan, R. Santillan and D. Castillo, *Chem. Heterocycl. Compd.*, 1999, **35**, 912.
- 20 T. A. Hopkins, K. Meerholz, S. Shaheen, M. L. Anderson, A. Schmidt, B. Kippelen, A. B. Padias, H. K. Hall, Jr., N. Peyghambarian and N. R. Armstrong, *Chem. Mater.*, 1996, **8**, 344.
- 21 X.-Y. Wang and M. Weck, *Macromolecules*, 2005, **38**, 7219.
- 22 M. Brinkmann, G. Gadret, M. Muccini, C. Taliani, N. Masciocchi and A. Sironi, *J. Am. Chem. Soc.*, 2000, **122**, 5147.
- 23 Y. L. Teng, Y. H. Kan, Z. M. Su, Y. Liao, L. K. Yan, Y. J. Yang and R. S. Wang, *Int. J. Quantum Chem.*, 2005, **103**, 775.
- 24 M. J. Frisch, G. W. T., H. B. Schlegel, G. E. Scuseria, M. A. Robb, J. R. Cheeseman, J. A. Montgomery, T. Vreven, K. N. Kudin, J. C. Burant, J. M. Millam, S. S. Iyengar, J. Tomasi, V. Barone, B. Mennucci, M. Cossi, G. Scalmani, N. Rega, G. A. Petersson, H. Nakatsuji, M. Hada, M. Ehara, K. Toyota, R. Fukuda, J. Hasegawa, M. Ishida, T. Nakajima, Y. Honda, O. Kitao, H. Nakai, M. Klene, X. Li, J. E. Knox, H. P. Hratchian, J. B. Cross, V. Bakken, C. Adamo, J. Jaramillo, R. Gomperts, R. E. Stratmann, O. Yazyev, A. J. Austin, R. Cammi, C. Pomelli, J. W. Ochterski, P. Y. Ayala, K. Morokuma, G. A. Voth, P. Salvador, J. J. Dannenberg, V. G. Zakrzewski, S. Dapprich, A. D. Daniels, M. C. Strain, O. Farkas, D. K. Malick, A. D. Rabuck, K. Raghavachari, J. B. Foresman, J. V. Ortiz, Q. Cui, A. G. Baboul, S. Clifford, J. Cioslowski, B. B. Stefanov, G. Liu, A. Liashenko, P. Piskorz, I. Komaromi, R. L. Martin, D. J. Fox, T. Keith, M. A. Al-Laham, C. Y. Peng, A. Nanayakkara, M. Challacombe, P. M. W. Gill, B. Johnson, W. Chen, M. W. Wong, C. Gonzalez and J. A. Pople, *Gaussian 03, Revision C.01*, Gaussian, Inc., Wallingford, CT, 2004.
- 25 A. D. Becke, *J. Chem. Phys.*, 1993, **98**, 5648.
- 26 C. Lee, W. Yang and R. G. Parr, *Phys. Rev. B*, 1988, **37**, 785.
- 27 H.-Y. Chen, Y. Chi, C. S. Liu, J.-K. Yu, Y.-M. Cheng, K.-S. Chen, P.-T. Chou, S.-M. Peng, G.-S. Lee, A. J. Carty, S.-J. Yeh and C.-T. Chen, *Adv. Funct. Mater.*, 2006, **15**, 567.
- 28 J. S. Binkley, J. A. Pople and W. J. Hehre, *J. Am. Chem. Soc.*, 1980, **102**, 939.
- 29 P. C. Hariharan and J. A. Pople, *Theor. Chim. Acta*, 1973, **28**, 213.
- 30 R. Bauernschmitt and R. Ahlrichs, *Chem. Phys. Lett.*, 1996, **256**, 454.
- 31 M. E. Casida, C. Jamorski, K. C. Casida and D. R. Salahub, *J. Chem. Phys.*, 1998, **108**, 4439.
- 32 R. E. Stratmann, G. E. Scuseria and M. J. Frisch, *J. Chem. Phys.*, 1998, **109**, 8218.
- 33 V. Barone and M. Cossi, *J. Phys. Chem. A*, 1998, **102**, 1995.
- 34 M. Cossi, N. Rega, G. Scalmani and V. Barone, *J. Comput. Chem.*, 2003, **24**, 669.
- 35 S. Miertus, E. Scrocco and J. Tomasi, *Chem. Phys.*, 1981, **55**, 117.
- 36 D. J. Parks, W. E. Piers and G. P. A. Yap, *Organometallics*, 1998, **17**, 5492.
- 37 D. Naumann, H. Butler and R. Gnann, *Z. Anorg. Allg. Chem.*, 1992, **618**, 74.